Ferroelasticity in phenothiazine: A Brillouin-scattering study

C. Ecolivet and M. Sanquer
Groupe de Physique Cristalline, Université de Rennes I, Campus de Beaulieu, 35042 Rennes-CÉDEX, France

K. Ishii and H. Nakayama
Department of Chemistry, Faculty of Sciences, Gakushuin University, Mejiro, Toshimaku, Tokyo, 171, Japan
(Received 6 November 1990)

The ferroelastic structural phase transition (SPT) and the elastic properties of the phenothiazine acoustic soft mode have been studied by Brillouin scattering. A pronounced softening of the C_{55}-related acoustic modes is observed for directions close to **a** or **c**, but a strong dispersion, with respect to ultrasonic results, is observed for the longitudinal-acoustic mode propagating along **c**. This dispersion and the behavior of C_{55} in the low-temperature phase are characterized by a value of the relaxation time of the order parameter at T_c in the 100-ps range, which suggests that the regime of this SPT is of the order-disorder type. Nevertheless the $C_{55}(T)$ variation in the low-temperature phase looks like that predicted in a true ferroelastic SPT.

I. INTRODUCTION

Only a few organic molecular crystals with van der Waals bonding are known to undergo ferroelastic structural phase transitions (SPT). Among them, acoustic soft modes have been observed by Brillouin scattering in malononitrile,[1] benzil,[2] sym-triazine,[3] and, recently, in *p*-dichlorodurene.[4]

Phenothiazine ($C_{12}H_8SN$) presents two phases: one monoclinic $P2_1/c$ (Ref. 5) at low temperatures and another one near room temperature. This phase was described as orthorhombic *Pnma* (Ref. 6), but a large thermal agitation, mainly due to a translation along the molecular long axis, led van de Waals and Feil[5] to propose that this structure was a "polysynthetic twinning" of a monoclinic cell. Their major argument was based on the possibility of finding two distinct possible locations of the phenothiazine molecule at each site, these locations being as far as 0.6 Å from each other. According to this proposition a SPT should not actually take place and more unusually, the high-temperature (HT) phase would be a twinned low-temperature (LT) phase.

However, the following studies revealed a more normal behavior. Typical differential scanning calorimetry (DSC) anomalies were recorded as well as Raman and optical signatures.[7] It was then shown that a first-order SPT relates these two phases, but without any large change in the unit-cell volume.

Such a ferroelastic SPT is characterized by a soft acoustic mode, which was only observed by ultrasonics in the HT phase due to domain attenuation below T_c.[8] These data and the Raman observations have been interpreted in the frame of a Landau theory where the primary order parameter is the crystalline strain e_5, as in a true ferroelastic SPT. However, this phenomenological theory does not explain the mechanism of this SPT and, even if the thermal agitation suggests a translational motion of the molecules along their long molecular axis, a microscopic explanation of this motion or a model still remains to be built.

In this paper, in Sec. II, we report about the elastic properties of the HT phase at room temperature and we relate them to the structure. In Sec. III, we study the evolution of all the diagonal elastic constants through the SPT even in the LT phase in presence of domains inside the scattering volume. In all the following, we refer to the crystallographic frame used by Nakayama and Ishii[9] where $c > b > a$.

II. EXPERIMENTAL AND ROOM-TEMPERATURE MEASUREMENTS

Single crystals were grown from refined phenothiazine according to a method which was described previously.[9] Crystals of good optical quality were (a,b) platelets with maximum dimensions $3\times2\times1$ mm^3, but, due to the softness of these crystals, they were used as grown in order to avoid damaging them. Low-temperature measurements were performed inside a cryostat working with a nitrogen flow, the temperature of which was stabilized to better than 0.1 K by a three-term regulation.

Brillouin-scattering experiments were performed with the interferometric system extensively described elsewhere,[10] but instead of an argon laser, we used a krypton one in order to avoid any heating of the scattering volume due to light absorption. Refractive indices of phenothiazine, needed in most of the Brillouin-scattering geometries, have been obtained from the ratio of the Brillouin shifts related to the same acoustic phonon measured in backscattering and in a smaller angle geometry where the refractive indices are removed from the Brillouin shift formula. At room temperature we obtained, at 647 nm,

$$n_a = 1.72, \quad n_b = 1.60, \quad n_c = 1.95$$

with uncertainties in the percent range.

More than 30 different directions were investigated at room temperature and 72 sound velocities were determined. We should stress here that velocities measured in the $(\mathbf{a},\mathbf{b})$ plane are independent of the refractive indices

TABLE I. Elastic constants in GPa at room temperature.

$C_{11}=8.09$
$C_{22}=8.87$
$C_{33}=15.76$
$C_{44}=2.52$
$C_{55}=0.25$
$C_{66}=5.28$
$C_{12}=5.97$
$C_{23}=4.46$
$C_{13}=2.61$

since they were all measured in the smaller angle geometry mentioned above. These 72 sound velocities were used for fitting the nine elastic constants of the orthorhombic system which are listed in Table I.

As in all molecular crystals made of rigid molecules interacting by van der Waals forces, compressional elastic constants are larger along the molecular long axis. Here also, C_{33} is nearly twice as large as C_{11} or C_{22}, which are related to the longitudinal waves propagating along two directions perpendicular to the molecular long axis. However, the phenothiazine molecule is not planar and one may doubt the validity of the rigid molecule scheme. In fact, we can compare with similar organic van der Waals materials, the closest examples are provided by the polyacenes series which have a monoclinic structure. In this series, longitudinal sound velocities perpendicular to the long axis are about 2500 m/s;[11] they are similar to velocities in phenothiazine along **a** and **b** and they also give elastic constants in the 8–9 GPa range. This range is quite typical of van der Waals crystals built of flat organic molecules since these values are also found in other series like the *p*-polyphenyls one.[12]

Although phenothiazine is a three-ring molecule, the longitudinal velocity along the long-axis direction is much closer to the naphthalene value (3500 m/s) than to the anthracene one (3900 m/s). But, due to the mass increase, mainly produced by the substitution of two carbon atoms by one sulfur and one nitrogen atom, it is wiser to compare elastic constants which do take into account density. In such a case, C_{33} in phenothiazine (~ 16 GPa) is an average between naphthalene (14.5 GPa) and anthracene (19 GPa) so that we may think that the effective compression modulus along this direction is reduced by the ability to fold the phenothiazine molecule along the *S*-*N* axis; this motion is related to the free internal vibration called the butterfly mode.

The smallest elastic constant is C_{55}, which corresponds to the soft mode and, since it was not directly measured, the accuracy on this constant is probably small. This can be understood by looking at Fig. 1, which displays the angular variation of sound velocities in the crystallographic planes. In particular, the angular variation of the C_{55} related modes is very steep near **a** or **c** so that the extrapolation towards **a** or **c** is not obvious. However, our value (0.25 GPa) is not far from the one measured directly by ultrasonics: 0.31 GPa.[13]

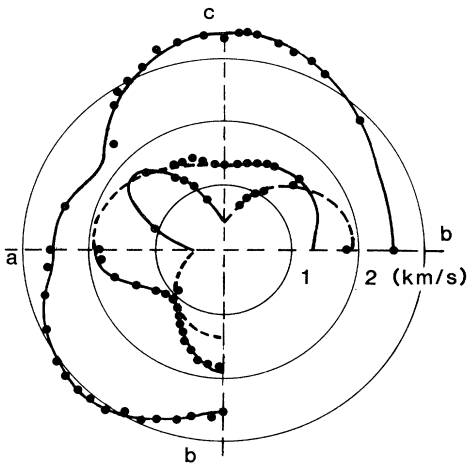

FIG. 1. Sound velocity in the (**a**,**b**), (**b**,**c**), (**a**,**c**) crystallographic planes at 293 K. Solid symbols represent experimental data and lines the best fit obtained with the elastic constant of Table I.

III. ELASTIC ANOMALIES AT THE FERROELASTIC SPT

Sound velocities corresponding to the diagonal elastic constants, as labeled from the prototype phase, have been measured between room temperature and 180 K. Probably due to some polarization leakage and a fast collecting optics ($f/4$), even transverse velocities have been measured in the backscattering geometry, which was used in order to enhance the scattered light by increasing the scattering volume.

In that geometry, crystals had to be slightly rotated from the normal incidence in order to avoid specular reflection by crystal surfaces into the interferometer. By measuring external reflection angles and applying the Snell-Descartes law to the crystal, we could determine, with a reasonable accuracy, the phonon propagation

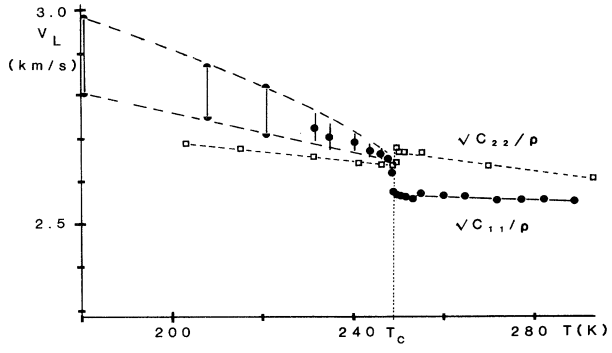

FIG. 2. Longitudinal sound velocities vs temperature for modes propagating along **a**, (C_{11}) and **b**, (C_{22}) directions. Split symbols and error bars refer to resolved and unresolved lines due to domains inside the scattering volume. Lines are guides for the eye.

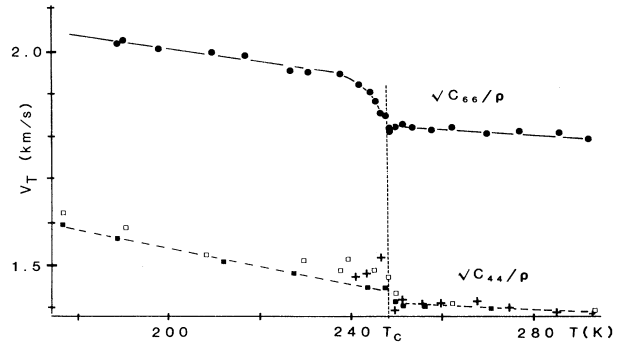

FIG. 3. Transverse sound velocities vs temperature for modes related to the C_{44} and C_{66} elastic constants. Different symbols for the C_{44} related mode are related to different experiments and are produced by domains inside the scattering volume. Lines are only guides for the eye.

directions inside the crystal. Moreover, the measured sound velocities could also be compared to the sound velocity diagrams for confirmation of the directions.

Figure 2 displays the evolution with temperature of the phase velocity of compressional waves along **a** and **b** computed with the room-temperature refractive indices. One can notice small discontinuities found at $T_c = 248.8 \pm 0.5$ K. As expected, domain effects are observable below T_c along **a**. Just below T_c this longitudinal Brillouin linewidth increases due to domains inside the scattering volume and finally splits into two resolved lines around 220 K as an effect of the lower symmetry of the low-temperature phase.

Figure 3 shows the temperature evolution of transverse sound velocities related to $\sqrt{C_{66}}$ and $\sqrt{C_{44}}$. They do not show large discontinuities, but the C_{44}-related mode is very sensitive to domains inside the scattering volume. This results in scattered data below T_c since contributions of different domains are not resolved.

Figure 4 compares the evolution of C_{33} from measure-

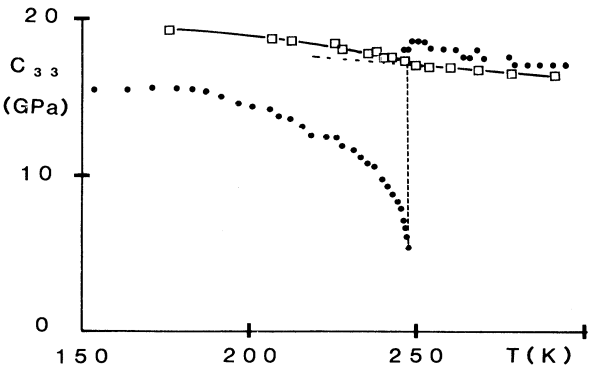

FIG. 4. Evolution of the elastic constant C_{33} vs temperature at 6.7 MHz (Refs. 8 and 13) (●) and at 18 GHz (□). The nearly horizontal dashed line extrapolates the high-temperature phase behavior.

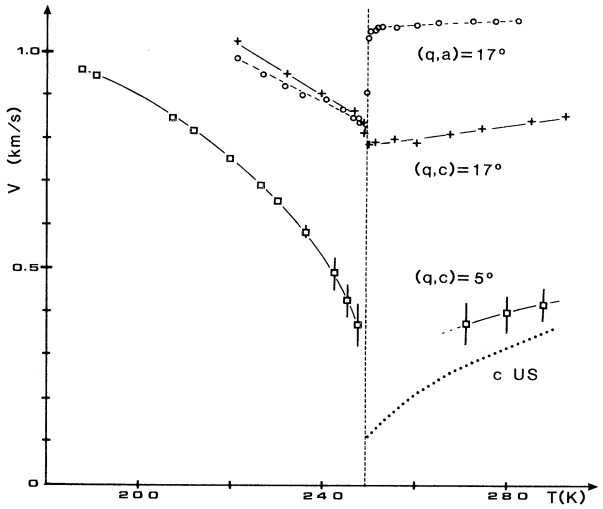

FIG. 5. Sound velocity vs temperature for modes related to C_{55} for different orientations. (**q**,**a**)=(**q**,**c**)=17° were obtained in the (**a**,**c**) plane whereas (**q**,**c**)=5° was measured in the (**b**,**c**) plane. The dotted line compares with ultrasonics results (Ref. 8). Lines are guides for the eye.

ment at about 18 GHz by Brillouin scattering and at 6.7 MHz by ultrasonics.[8,13] At lower frequencies this elastic constant exhibits an exceptionally large step of 13 GPa, whereas Brillouin-scattering experiments only reveal a slight change of slope at T_c.

In Fig. 5, several measurements of the sound velocity of the soft mode, which is related to C_{55}, are displayed with, for comparison, ultrasonic measurements of this mode in the high-temperature phase.[8] As it can be seen on the room-temperature sound velocity diagrams, the angular dispersion is very strong near the **a** and **c** directions. This confirms the softening of a unique elastic constant C_{55}. The closest direction to **c** which allowed a soft-mode observation, was obtained at 5° of **c** in the (**b**,**c**) plane. Along this direction, the transverse sound velocity is in reasonable agreement with ultrasonic measurements although our accuracy is small for velocities lower than 500 m/s due to an intense Rayleigh line. Nevertheless, it is obvious that this sound velocity should not decrease continuously to zero at T_c.

Directions at 17° from **a** and from **c** were investigated in the (**a**,**c**) plane; if they do show a definite softening at T_c in both phases, they also show some extra features which are not related to C_{55} and which should be explained.

IV. DISCUSSION

Since surfaces of the samples were rotated in order to avoid specular reflection, we must try to evaluate errors introduced by this technique. For small angles, we will develop sound velocities with respect to the angle defined by the scattering wave vector **q** and the principal crystallographic directions. According to the sound velocity di-

agrams in the principal crystallographic planes, the effect of this sample rotation is certainly negligible for longitudinal modes but is of extreme importance for the C_{55}-related modes.

Let us first examine what occurs in the (**b**,**c**) plane. In that plane the C_{55}-related mode is a true transverse mode which has a velocity V_T described by

$$\rho V_T^2 = C_{55} n_z^2 + C_{66} n_y^2 , \tag{1}$$

where ρ is the density and n_y and n_z are the cosines of the propagation direction **q**.

If we develop this expression here with respect to φ, the direction angle with **c**, we obtain, in the neighborhood of **c**,

$$\rho V_T^2(\varphi) \simeq C_{55} + C_{66}\varphi^2 . \tag{2}$$

For $\varphi = 5°$, if we ignore C_{66}, we obtain, for the C_{55} related velocity, a value which is overestimated by 60 m/s near room temperature and never by more than 70 m/s at lower temperatures if we refer to the C_{66} variations drawn in Fig. 3. In the LT phase, C_{66} actually represents a combination of the monoclinic C_{66}, C_{46}, and C_{44}.

In the (**a**,**c**) plane the situation is quite different since the C_{55}-related modes are quasitransverse (QT) modes which have velocities defined by

$$2\rho V_{\mathrm{QT}}^2 = \Gamma_{11} + \Gamma_{33} - [(\Gamma_{11} - \Gamma_{33})^2 + 4\Gamma_{13}^2]^{1/2} , \tag{3}$$

where, in the orthorhombic phase,

$$\begin{aligned} \Gamma_{11} &= C_{11} n_x^2 + C_{55} n_z^2 , \\ \Gamma_{33} &= C_{55} n_x^2 + C_{33} n_z^2 , \\ \Gamma_{13} &= (C_{13} + C_{55}) n_x n_z . \end{aligned} \tag{4}$$

By an expansion of ρV_{QT}^2 in powers of φ near **a** or **c**, one gets close to the **a** direction,

$$\rho V_{\mathrm{QT,a}}^2 \simeq C_{55} + \left[C_{33} - \frac{(C_{13}+C_{55})^2}{C_{11}-C_{55}} \right] \varphi^2 + \left[\frac{10 C_{13}^2}{C_{11}} - C_{55} \right] \frac{\varphi^4}{3} \tag{5}$$

and close to **c**,

$$\rho V_{\mathrm{QT,c}}^2 \simeq C_{55} + \left[C_{11} - \frac{(C_{13}+C_{55})^2}{C_{33}-C_{55}} \right] \varphi^2 + \left[\frac{10 C_{13}^2}{C_{33}} - C_{55} \right] \frac{\varphi^4}{3} . \tag{6}$$

Since, even for $\varphi = 17°$, the φ^4 terms in expansions (5) and (6) have negligible values, it means that these equations can provide for a good approximation of the velocity of the QT mode in the neighborhood of **a** and **c**. The φ^2 terms correspond, at room temperature, to an addition to the C_{55} contribution to the QT phase velocity of 980 m/s along (**a**−17°) and 750 m/s along (**c**−17°). These values are remarkably close to the minimum values recorded just above T_c along these directions, 1020 and 785 m/s, respectively, in agreement with a nearly vanishing C_{55}.

We are now able to understand the variation of the sound velocities of these QT modes recorded along (**a**−17°) and (**c**−17°) since, by dropping numerically unimportant terms in Eqs. (5) and (6), one obtains, in the vicinity of T_c ($T \geq T_c$),

$$\begin{aligned} \rho V_{\mathrm{QT,a}}^2(T) &\simeq C_{55}(T) + C_{33}(T)\varphi^2 , \\ \rho V_{\mathrm{QT,c}}^2(T) &\simeq C_{55}(T) + C_{11}(T)\varphi^2 . \end{aligned} \tag{7}$$

These equations do show that the measured velocity variations are due to mixing of the $C_{55}(T)$ slope with the $C_{33}(T)$ or $C_{11}(T)$ variations reduced by the factor φ^2. If we still always assume that monoclinic terms C_{15} and C_{35} are negligible in the vicinity of T_c ($T < T_c$) we, first, obviously see the similarity between $V_{\mathrm{QT,c}}(T)$ and $\sqrt{C_{11}(T)/\rho}$, and second, we can try to relate $\rho V_{\mathrm{QT,a}}^2(T)$ to the $C_{33}(T)$ curve obtained by ultrasonics. In the close vicinity of T_c, the step observed on $\rho V_{\mathrm{QT,a}}^2$ is equal to $\varphi^2 \Delta C_{33}$ if no dispersion occurs. Since $\Delta(\rho V_{\mathrm{QT,a}}^2) \simeq 0.34$ GPa, we obtain $\Delta C_{33} \simeq 3.5$ GPa at 6 GHz, which is an intermediate value between 13 GPa at 6 MHz and almost zero at 20 GHz. Thus, there is a strong dispersion in the GHz frequency range and our derivation of ΔC_{33} will be frequency dependent.

Another question arises when looking at Fig. 6, which shows C_{55} versus temperature in the LT phase. In this figure we notice that the linearity range cannot exceed 15 K, even with the poor accuracy of the two lowest experimental points, whereas in the prototype phase, C_{55} exhibits a linear behavior in a 50-K range above T_c. The interpretation of all these anomalies requires a more precise interpretation of our data and this can be provided for by a Landau theory.

Using a free-energy expansion where the primary order parameter is the e_5 shear strain, which may be bilinearly coupled to an optic mode of coordinate Q and quadratically coupled to the non-symmetry-breaking strain e_3 which seems to be the only one involved, we may write

$$F - F_0 = \frac{\alpha}{2}(T - T_0)e_5^2 + \frac{B}{4}e_5^4 + \frac{D}{6}e_5^6 + \tfrac{1}{2}kQ^2 - \lambda e_5 Q + \tfrac{1}{2}C_{33}e_3^2 - \frac{K}{2}e_5^2 e_3 . \tag{8}$$

Under equilibrium conditions, one obtains, for a first-order SPT with $T_1 = T_0 + \lambda^2/\alpha k$ and $T_c = T_1 + 3B'^2/16D\alpha$,

$$e_5^2 = -\frac{B'}{2D}\left[1 + \left[1 + \frac{3}{4}\frac{T_1 - T}{T_c - T_1} \right]^{1/2} \right] , \tag{9}$$

where T_1 is the stability limit of the HT phase and $B' = B - K^2/2C_{33}$ is negative. We should also notice that B could be positive since the static anomaly related to C_{33} is very large. In the HT phase, C_{55}^+ is linear versus temperature, whereas in the LT phase

$$C_{55}^{-}=\frac{3B'^2(T-T_1)}{16(T_c-T_1)D} \quad (T>T_c)\ . \tag{10}$$

In the LT phase, we may obtain an elastic response within the two limits corresponding, first to a dynamic equilibrium between the e_3 and e_5 fluctuations and, second, to the case where the strain and the order-parameter fluctuations cannot reach equilibrium due to a non-negligible order-parameter relaxation time.[14] This last situation is often involved in explaining large slope ratios of optical soft modes between the high- and low-temperature phases, but, in that case, the origin may lie in the absence of elastic fluctuations at such high frequencies.

In the first case the elastic constant is obtained by a constant stress derivative,

$$\begin{aligned} C_{55}^{0}&=\left[\frac{\partial^2\Delta F}{\partial e_5^2}\right]_{\sigma_3=0} \\ &=\left[\frac{\partial^2\Delta F}{\partial e_5^2}\right]_{e_3}-\left[\frac{\partial^2\Delta F}{\partial e_5\partial e_3}\right]^2\left[\frac{\partial^2\Delta F}{\partial e_3^2}\right]_{e_5}^{-1} \\ &=\frac{B'^2}{D}(V+\sqrt{V})\ , \end{aligned} \tag{11}$$

where $V=1+\frac{3}{4}(T_1-T)/(T_c-T_1)$, whereas the second limit is obtained by a constant strain derivative

$$\begin{aligned} C_{55}^{\infty}&=\left[\frac{\partial^2\Delta F}{\partial e_5^2}\right]_{e_3} \\ &=\frac{B'^2}{D}\left[V+\sqrt{V}-\frac{K^2}{2C_{33}B'}(1+\sqrt{V})\right]\ . \end{aligned} \tag{12}$$

Then the ratio of the slopes of C_{55} versus temperature in both phases should be found between

$$\frac{dC_{55}^{\infty}/dT}{dC_{55}^{+}/dT}=-4\left[1+\frac{1-K^2/2B'C_{33}}{2\sqrt{V}}\right] \tag{13}$$

and

$$\frac{dC_{55}^{0}/dT}{dC_{55}^{+}/dT}=-4\left[1+\frac{1}{2\sqrt{V}}\right]\ .$$

This same coupling also modifies C_{33}. In the case of a dynamic equilibrium, it gives a negative step

$$\Delta C_{33}(T)=-\frac{K^2}{2[B-B'(1+\sqrt{V})]}\ , \tag{14}$$

whereas, in the other case, this anomaly does not exist and C_{33} is temperature independent, in a first approximation.

Due to the first-order character of this transition, the relative step at T_c equals

$$\Delta C_{33}(T_c)/C_{33}=\frac{1}{1-B'C_{33}/K^2}\ . \tag{15}$$

According to ultrasonic data $0.70<\Delta C_{33}/C_{33}<0.75$, this gives, at T_1,

$$8.9<\left|\frac{dC_{55}^{\infty}/dT}{dC_{55}^{+}/dT}\right|_{T_1}<9.4$$

and

$$\left|\frac{dC_{55}^{0}/dT}{dC_{55}^{+}/dT}\right|_{T_1}\simeq 6\ ,$$

but a poor experimental accuracy gives a ratio of 6 ± 4. However, at T_c-20 K, the same theoretical ratios are 4.95 and 5.05, respectively, whereas the measured ratio is equal to 4.53. One should also notice that we use, in the experimental ratio, data from different origins: ultrasonics and light scattering. This could also explain some discrepancies between measurements and theoretical pre-

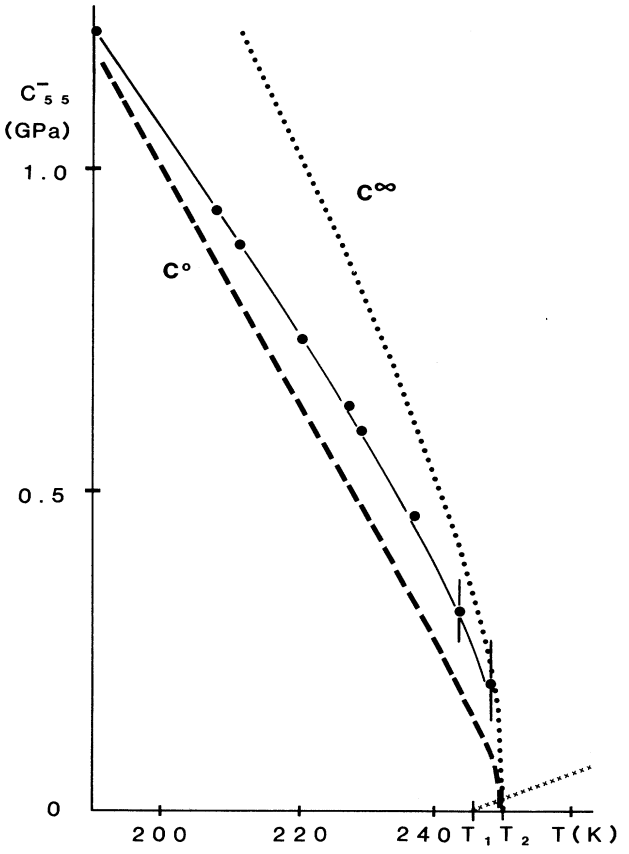

FIG. 6. Evolution of C_{55}^{-} vs temperature. C_{55}^{+} (high-temperature phase) is represented by small crosses in the lower right part of the figure. The dotted and dashed lines represent, respectively, the two limits C_{55}^{∞} and C_{55}^{0} computed from ultrasonic data (Ref. 8) and Eqs. (12) and (11). Experimental points are large circles with error bars for temperatures where the Brillouin lines are in the wing of the Rayleigh line. T_1 and T_2 are the spinodal temperatures for the HT and LT phases. The solid line is only a guide for the eye.

dictions, but we will show that the differences in the slopes have a physical origin.

We can see in Fig. 5 that the velocity of the C_{55}-related mode at (**c**−5°) does not exhibit any splitting. It means that, in the low-temperature phase, this direction is close to the direction where the velocity of the soft acoustic mode is minimum, so that we can assimilate ρV_{QT}^2(**c**−5°) to C_{55}^-.

Figure 6 displays the variation of C_{55}^- versus temperature and compares it to C_{55}^0 and C_{55}^∞, which have been computed from ultrasonic data[8] $T_c - T_1 = 3.5$ K, $T_c = 248.7$ K, $B'^2/2D = 72\times10^6$ N m^{-2}, $K^2/2B'C_{33} = -1.5$. We clearly see in this figure that our C_{55}^- measurement occurs in two different regimes. At low temperatures, where the relaxation time is not diverging, our result is close to C_{55}^0, whereas in the vicinity of T_c our measured values are much closer to C_{55}^∞ since the relaxation time diverges at T_2 the spinodal temperature of the LT phase.

If one assumes a single relaxation time τ for the order parameter, one may write

$$C_{55}(\omega,T) = C_{55}^\infty - \frac{C_{55}^\infty(T) - C_{55}^0(T)}{1+\omega^2(T)\tau^2(T)} , \tag{16}$$

where $\omega(T)$ is the measured Brillouin shift.

It is then possible to estimate the only unknown quantity $\tau(T)$ from this formula [Eqs. (11) and (12)], ultrasonic data and Brillouin shifts. Near T_c, τ is found to be close to 100 ps, whereas it falls down to 10 ps at $T_c - 40$ K. Its variation looks like $(C_{55}^0)^{-1}$ (Fig. 7).

Within the same Landau-Khalatinkov scheme (see, for example, Ref. 15), we may also study the C_{33} variations:

$$C_{33}(T,\omega) = C_{33} - \frac{K^2\tau}{\Gamma e_5^2(1+\omega^2\tau^2)} , \tag{17}$$

where $\tau^{-1} = C_{55}^0$, Γ being a constant defining the rate of return towards equilibrium.

If we compare the magnitude of $\Delta C_{33}(T_c)$ at 6.7 MHz and 6 GHz, we conclude that $\tau(T_c)$ should be close to 100 ps in excellent agreement with the estimation based on the C_{55} variation. If we try to use the Brillouin-scattering data at 6 GHz and the ultrasonic data at 6.7 MHz, we obtain another determination of $\tau(T_c)$ lying close to 50 ps, but, due to the mixing in Eq. (7) of the elastic constant C_{55} with C_{33}, which is multiplied by a small parameter, this value is probably less reliable. Nevertheless, this range of $\tau(T)$ indicates that the dispersions of C_{55} and C_{33} have the same origin, i.e., the relaxation of the order parameter.

Let us stress here that the value of

$$\frac{\Delta C_{33}(T_c)}{C_{33}} \simeq 0.75$$

directly implies that $B' \simeq -2B$, and since the observed behavior is discontinuous, it means that, without the $e_5 - e_3$ coupling, this SPT would have actually been continuous. One can even think to the possibility of observing second-order or tricritical behavior by clamping this crystal.

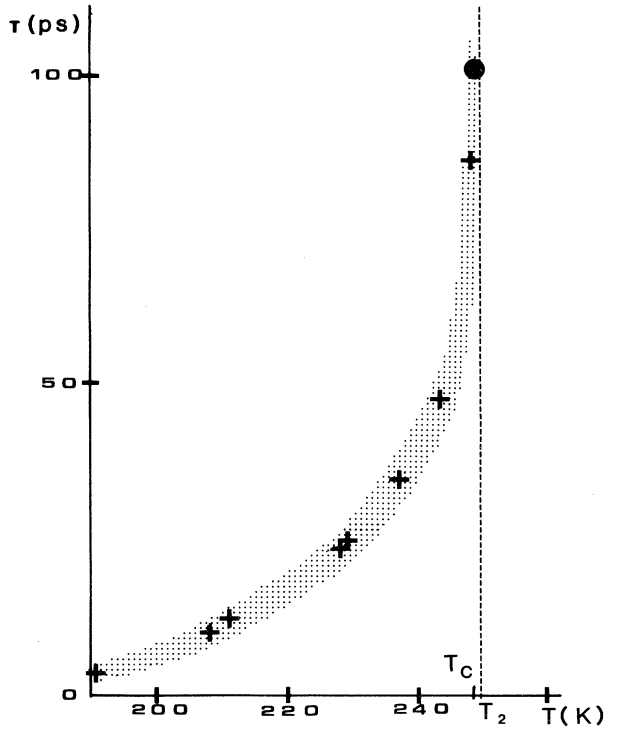

FIG. 7. Evolution of the relaxation time of the order parameter. + represent values computed from Eq. (16), whereas the large circle comes from the disperson of C_{33} between 6.7-MHz experiments and Brillouin backscattering [Eq. (17)].

V. CONCLUSION

In this Brillouin-scattering study, we have shown that the room-temperature elastic properties reflect the structure of the crystal with a larger elastic constant C_{33} along the molecular long axis, although a higher value would have been expected from the comparison with naphtalene and anthracene molecules. This relative softness is probably due to a coupling of elastic waves to internal "butterfly modes."

The temperature dependence of all the diagonal elastic constants referred to the orthorhombic frame show some typical anomalies. Along **a**, the longitudinal Brillouin line splits in two components in the LT phase under the influence of the new elastic constant C_{15}. Along **c**, a very strong quadratic coupling between the strain e_3 and the order parameter generates, at T_c, a dramatic softening of C_{33} observed at 6.7 MHz, but this softening is invisible above 18 GHz.

The magnitude of this coupling is so large that it is, to our knowledge, the first example of a SPT in a molecular crystal where it is directly proved that the coupling of the order parameter with a totally symmetric strain produces a first-order behavior.

The investigations of the frequency dependence of C_{33} and of the temperature dependence of C_{55} have proved that their behavior can be coherently described by a sin-

gle relaxation time which diverges, at T_2, the spinodal temperature of the low symmetry phase. Measurements of $\tau(T_c)$ in the 100-ps range, or even a value of $\tau=10$ ps at (T_c-40 K) preclude the interpretation of any optical mode in the 10-cm^{-1} range ($\Omega\simeq 2\times 10^{12}$ rad s^{-1}) as a soft optic mode, since $\Omega\tau$ would be much larger than unity and, consequently, fluctuations would be overdamped.

We can then assert that this SPT is not driven by an optical soft mode and confirm the analysis of the mode labeled 3 in Ref. 9 by a hard mode biquadratically coupled to the order parameter. Moreover, the evolution with temperature of some Raman linewidths supports the idea of an order-disorder regime.

The major remaining problem about this SPT is the nature of its driving force: Is it a pure ferroelastic SPT where strain is the primary order parameter or a ferroelasticity induced by a relaxing optical phonon? In our analysis we did not use at all the optical phonon coordinate Q of Eq. (8), so, we can think of this SPT as a true ferroelastic one. Otherwise, one may ask if the temperature range where C_{55} varies linearly in the high-temperature phase extends significantly beyond room temperature because a large coupling between an optical mode and a shear strain may also give a limited temperature range where C_{55} would vary linearly.

In order to improve our knowledge of this SPT, we plan new experiments with different crystals so that different scattering geometries could provide for direct observations of the elastic anomalies at different frequencies instead of indirect measurements.

ACKNOWLEDGMENT

Groupe de Physique Cristalline is Unité de Recherche Associée au Centre National de la Recherche Scientifique (CNRS), France (Contract No. 040804).

[1]Y. Higashigaki and C. H. Wang, J. Chem. Phys. **71**, 3813 (1979).
[2]R. Vacher, H. Boissier, and J. Sapriel, Phys. Rev. B **23**, 215 (1981).
[3]A. Yoshihara, W. D. Wilber, E. R. Bernstein, and J. C. Raich, Phys. Rev. B **76**, 3218 (1982).
[4]C. Ecolivet, L. Toupet, Ph. Bourges, and B. Jakubowski, Ferroelectrics **109**, 75 (1990).
[5]B. W. van de Waals and D. Feil, Acta Crystallogr. B **33**, 314 (1977).
[6]J. J. H. McDowell, Acta Crystallogr. B **32**, 5 (1976).
[7]H. Nakayama, K. Ishii, E. Chijiwa, M. Wada, and A. Sawada, Solid State Commun. **55**, 59 (1985).
[8]H. Nakayama, K. Ishii, and A. Sawada, Solid State Commun. **67**, 179 (1988).
[9]H. Nakayama and K. Ishii, Chem. Phys. **114**, 431 (1987).
[10]C. Ecolivet, M. Sanquer, J. DeWitte, and R. Pellegrin, J. Chem. Phys. **78**, 6317 (1983).
[11]A. I. Kitaigorodski, *Molecular Crystals and Molecules* (Academic, New York, 1973).
[12]C. Ecolivet, J. Phys. (Paris) Colloq. **42**, C6-578 (1981).
[13]N. Morita, H. Nakayama, and K. Ishii, J. Phys. Soc. Jpn. (to be published).
[14]R. A. Cowley, Adv. Phys. **29**, 1 (1980).
[15]H. Z. Cummins, Phys. Rep. **185**, 211 (1990).